Shear Assessment of a Reinforced Concrete Bridge Deck Slab According to Level-of-Approximation Approach

Jiangpeng Shu[1,2*]

[1] Postdoctoral Fellow. Department of Structural Engineering, Norwegian University of Science and Technology, 7491 Trondheim, Norway. Email: Jiangpeng.shu@ntnu.no; Tel: +47 73 41 32 84
[2] Postdoctoral Researcher. Department of Architecture and Civil Engineering, Chalmers University of Technology, 412 96 Gothenburg, Sweden.

1 Abstract

Reinforced concrete (RC) slabs without shear reinforcement are commonly used for existing bridge structures. For such structures, shear and punching can be the governing failure mode at the ultimate limit state if subjected to large concentrated loads. The aim of this study is to examine a structured approach for the analysis of the RC bridge deck slabs, which make up a considerable proportion of the currently used bridge decks. The method used for analyses is the levels-of-approximation introduced in fib Model Code for Concrete Structures 2010 (MC2010). The different levels include simplified calculation method, linear finite element analysis as well as non-linear finite element analysis. The differences between analysis methods at different levels of analyses were discussed regarding one-way shear and punching shear behaviour of the slab.

Key words: Shear and punching, Level-of-Approximation, Bridge deck slab, FE analysis, Full-scale test

2 Introduction

Existing infrastructure represents a substantial part of societal assets and existing bridges represent a huge capital that needs to be well administrated [1,2]. Reinforced concrete (RC) bridge deck slabs are among the most exposed bridge parts and are often critical to damage [3]. One-way shear and punching shear may be the governing failure mode in RC slabs without shear reinforcement when subjected to large concentrated loads. Currently, building codes of practice, such as ACI 318-14 [4] and EC 2 (Eurocode 2) [5], provide several approaches to check the shear strength of concrete slabs. However, previous studies have shown that existing models provided by design provisions are too conservative and that enhanced assessment methods can reveal higher load-carrying capacity [1].

In general, the assessment of bridge structure can be classified into three different aspects, i.e. the model sophistication, information of the structure as well as the uncertainty consideration. The engineers need more improved information about the structure to develop a more sophisticated structural model, with consideration of the level of modelling uncertainty in order to analyse the existing structure. [6] Thereafter, a decision support system is needed regarding if and how the assessment should be enhanced with respect to the three aspects in a systematic way [7].

In MC2010 (Model Code for Concrete Structures 2010) [8], a new approach, providing flexible, consistent and easy to use code provision, the level-of-approximation (LoA) approach is provided, where the accuracy of prediction of structural behavior can be progressively refined through a better estimation of the parameters involved in the assessment; see Figure 1. The accuracy in the estimate of the various physical parameters is refined in each new level by devoting more time to the analyses, so that the accuracy in the behaviour and strength provided by the equations is also improved. The LoA approach provides the engineering community for using successively improved structural analysis methods for enhanced assessment.

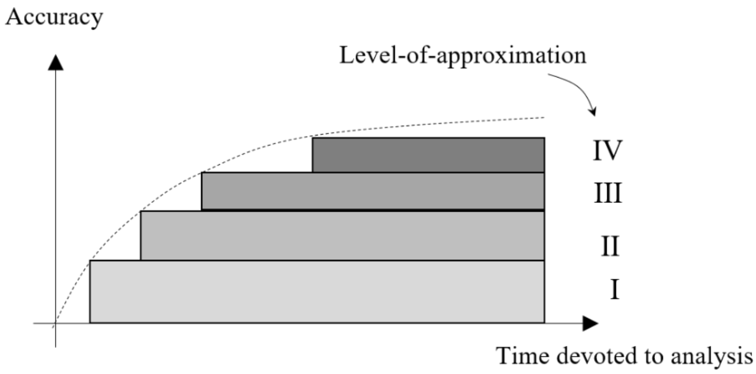

Figure 1. Accuracy on the estimate of the actual behaviour as a function of time devoted to the analysis for various levels-of-approximation [8].

The LoA approach allows the shear and punching capacities to be calculated for different "levels of approximation." [8] As the LoA increases, the required computational time and effort also increases, and the solution is expected to be a closer approximation of the sectional capacity. In all cases, a margin of safety is taken into account. For example, for the calculation of the sectional capacity of members without shear reinforcement, MC2010 [8] allows two lower levels of approximation. A similar consistent approach has been introduced for the sectional capacity of members with shear reinforcement and for the punching shear capacity based on the Critical Shear Crack Theory (CSCT) [9].

The aim of this study was to examine the LoA approach according to MC2010 [8] and modelling methods developed by Shu et al. [10], on a field tested bridge deck structure [11], for assessment of and to investigate the response of an existing real structure in engineering practice. The full-scale field test has been carried out on a 55-year RC bridge; the deck slab was subjected to concentrated load near one of the main girders, which led to a shear type failure of the slab. The LoA approach was then used to evaluate the capacity and response of the slab with respect to one-way shear and punching shear capacity. Accordingly, the one-way shear and punching shear resistance was calculated based on MC2010 [8], and with non-linear FE analyses. The difference between the assessment methods at different levels was discussed. Furthermore, the difference of failure modes between pure one-way shear and punching shear was discussed and a recommendation for engineering practice was provided.

3 Literature Review

Except for the LoA approach proposed in MC2010 [8], the principle has also been adopted for calculation of shear and punching capacity in literatures from different countries [12], e.g. Germany [13,14], Austria [15] and Czech [16], Sweden [17,6] and the Netherland [12]. The calculation methods form the MC2010 [8] have been applied for the shear and punching strength of RC slabs in different cases. For instance, Belletti et al. [18,19,20] applied it on shear strength of RC slabs and used non-linear FE analysis results coming from shell modelling combined with CSCT failure criterion [21] at higher level. Zoran et al. [22] studied punching shear resistance of column footings and foundation slabs and investigated how individual characteristics of the footings and of the soil affect the punching bearing resistance.

Not only for conventional RC slabs, the LoA approach from MC2010 [8] was also applied on punching strength of flat plates reinforced with Ultra High Performance Concrete (UHPC) and double-headed studs [23]. The influence of prestressing on the punching shear strength of members without shear reinforcement has been investigated by using LoA approach, and compared with EC 2 [5] and ACI 318-11 [4], by Thibault et al. [24] In terms of extreme accidental loading, Ruiz et al. [25] applied this approach for consistent design of concrete structures under fire conditions. This allows keeping simple rules for most cases but provides a general frame for assessing complex or sensitive structures. In addition, it does not only incorporate calculation methods, but specifies which ductility requirements are to be fulfilled in order to ensure a correct applicability of each method. Micallef et al. [26] used the higher level calculation method for punching shear on to flat slabs subjected to impact loading, considering the dynamic punching shear capacity and the dynamic shear demand.

When it comes to the higher LoA, according to previous studies, non-linear FE analysis is able to predict one-way shear and punching shear capacity of RC slabs with a high degree of accuracy. Examples of such non-linear FE analyses using 2D continuum element models can be found in Menetry et al. [27] and Hallgren [28], using 3D shell element modes in Marzouk & Chen [29] and Polak et al. [30]. Recommendations study concerning 3D shell elements were also presented in Shu et al. [10,31]. Guidelines for non-linear FE analysis also published by Rijkswaterstaat [32]. Based on these studies, it was concluded that not only the one-way shear and punching shear capacity could be predicted, but also that the influence of parameters such as specimen size and the amount of flexural reinforcement was reflected in the non-linear FE analysis. However, all studies mentioned above were mainly based on, and the developed models were applied to, laboratory experiments. In the past, only a limited number of the bridges deck slabs has been tested to failure, e.g. Miller et al. [33] and Pressley et al. [34]. Recently, a deck slab of Ruytenschildt Bridge was tested to failure by Lantsoght et al. [35], but the failure mode turned out to be due to bending even though calculation results with current building codes [5] showed that shear failure would occur. Therefore, the application of such approach to structures in reality is scarce and thus their suitability and advantage are yet to be examined.

4 Destructive test on the bridge deck slab

4.1 Bridge description

A two-lane road viaduct, constructed in 1959, was taken out of service due to urban transformation of the city of Kiruna in northern Sweden; see Figure 2 (*a*). Mining activities adjacent to the city have caused large ground deformations. A city transformation project was initiated to move Kiruna, including the infrastructure, to new safe areas unaffected by these ground deformations. Since 2006, the Kiruna Bridge had been monitored, in order to ensure its structural safety and keep it in service.

The configuration and dimensions of the bridge are presented in Figure 2 (*b*) and (*c*). With a total length of 121.5 m across five spans, the cast-in-situ superstructure of the bridge was composed of three continuous, longitudinal prestressed concrete (PC) girders, connected by non-prestressed RC cross-beams with a deck slab on the top. The girders were 1923 mm high and 410 mm wide, increasing to 650 mm at supports and to 550 mm at casting joints with the anchorage of prestressed reinforcement in span 2 and span 4. The bridge deck was 14.9 m wide, with additional 300 × 300 mm^2 edge beams on both sides, and 220 mm thick, gradually increased over a distance of 1.0 m to a thickness of 300 mm at the intersection to the girders. At the abutments, the superstructure was placed on bearings, whereas the intermediate supports consisted of RC columns. The area within the red dash line indicates the studied slab. The layout of the primary reinforcement in the bridge deck slab is shown in Figure 2 (*d*), with specified reinforcement bar diameters and center-to-center distances given by construction drawings.

Part of the material properties was obtained from in-situ tests, see Table 1. According to the tensile tests of reinforcements, the mean values of the yielding and ultimate tensile strength, were 584 MPa and 831 MPa for the 16 mm bars. Moreover, 25 cylinder concrete samples (with diameter of 100 mm and 200 mm) were taken from the bridge (7 from the slab, 11 from the girders and 7 from the columns), indicating an average value of the cylinder compressive strength of 62.2 MPa and a modulus of elasticity of 32.1 GPa. The tested material properties of reinforcing steel was also listed in Table 1.

Table 1. Material properties was obtained from in-situ tests.

Material parameters	Value
Compressive strength of concrete	f_{cm} = 62.2 MPa
Modulus of elasticity of concrete	E_{cm} =32.1 GPa
Yield and ultimate strength of reinforcing steel	f_{ym} = 584 MPa f_{um} = 831 MPa
Modulus of elasticity of reinforcing steel	E_{sm} = 200 GPa

Before demolition, the condition and structural behavior of the bridge were studied within a research project for the aim of developing methods for improved bridge assessment. There were no sign of corrosion, wear or any other damage to the slab prior to the test [11].

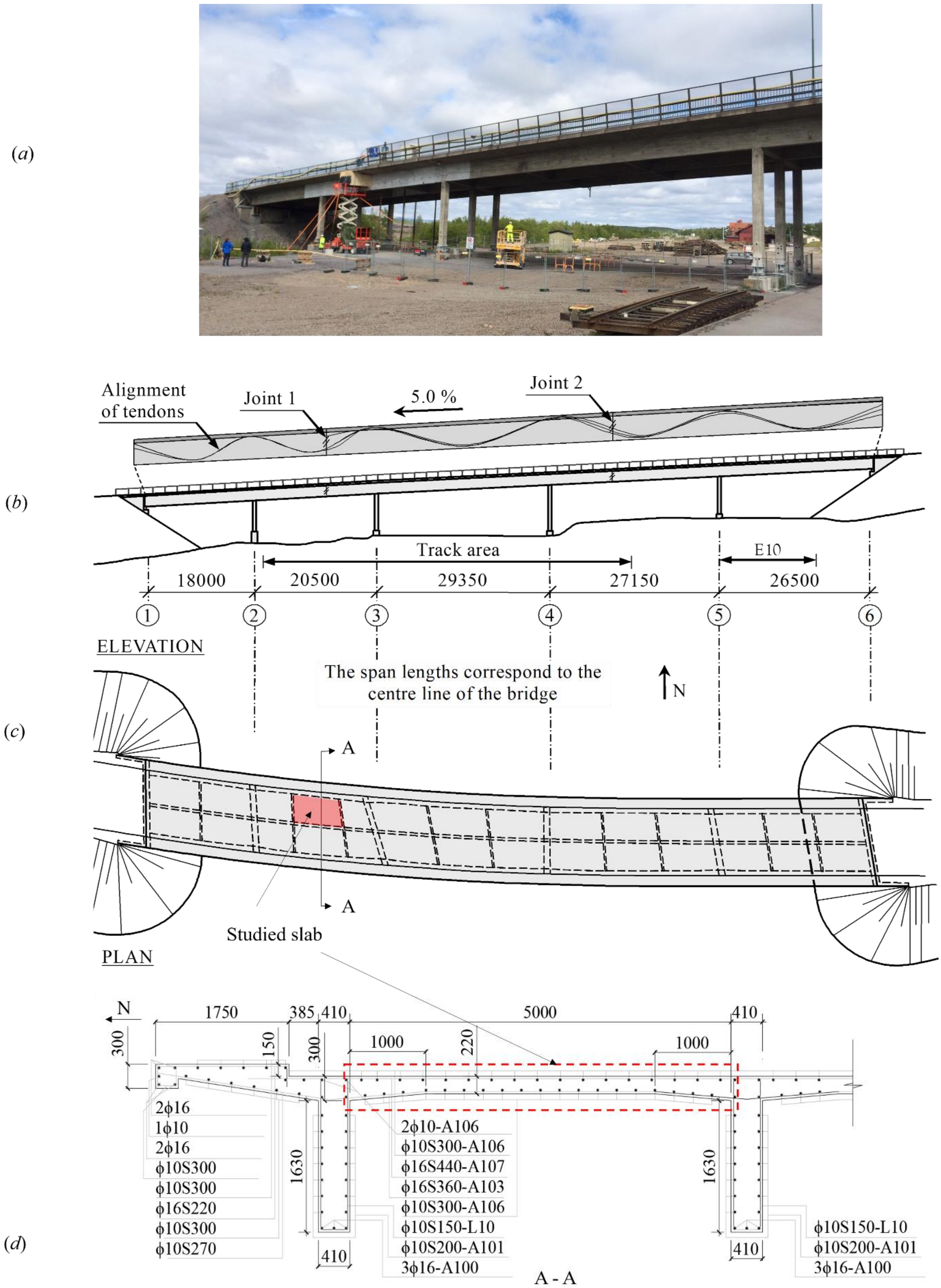

Figure 2. (*a*) Photo of the bridge; (*b*) Elevation of the bridge (*c*) Plan of the bridge (*d*) Cross section of the bridge girder and deck, as well as the layout of reinforcement. The slab inside the red line indicates the studied slab; unit: mm.

4.2 Destructive test

At an age of 55 years in 2014, the bridge was subjected to an extensive in-situ field destructive test program. In Figure 3 (*a*)-(*c*) the test setup for loading the bridge deck slab to failure is shown. The test load setup and dimension of the loading plate is determined according to Load Model 2 in EC 1 [36]. A single axle load applied on specific tire contact areas which covers the dynamic effects of the normal traffic on short structural members. The dimension of the loading plate, which has been presented in Figure 3 (*c*), is corresponding to the tire contact area. The load was applied to the bridge, using a longitudinally positioned simply supported load distribution beam and a forced-controlled hydraulic jack supported by wire thread through a drilled hole in the deck slab and anchorage in the bedrock. At the supports of the load distribution beam, 2.0 m apart, the load was transferred to the upper surface of the bridge deck slab (paving removed) through under-grouted steel plates. The positions of the loading plates are shown in Figure 3 (*c*). The loads are named as Load 1, which is further to the girder, and Load 2, which is closer to the girder.

In order to monitor the structural behavior of the bridge during the test, applied force and deflections were measured; see Figure 3 (*c*). The force was derived from the oil pressure in the hydraulic jack and draw-wire sensors were instrumented to the bridge to measure deflections relative to the ground. Deflections were measured at the bottom surface of the deck slab centrically underneath the load application and at the corresponding longitudinal position at the base of the adjacent girder. Moreover, the midspan deflection was measured for each girder.

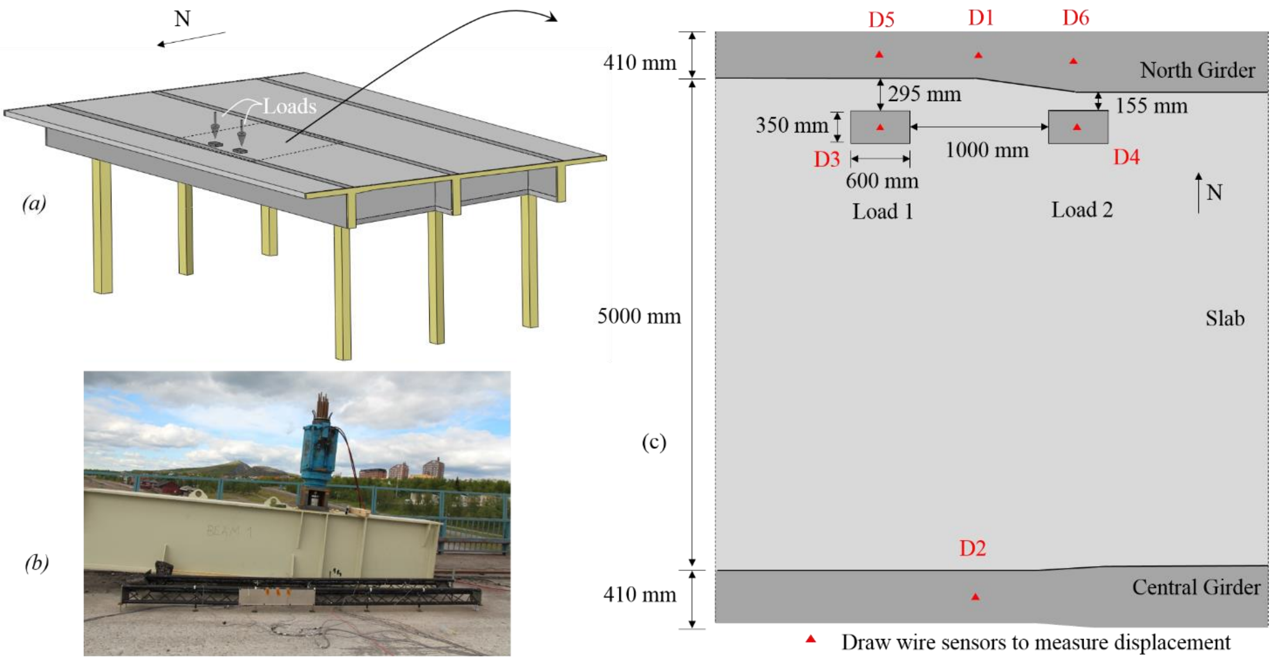

Figure 3. (*a*) Isometric view of layout of loading plates, (*b*) photo of field test, loading beam and hydraulic jack, and (*c*) layout of loading plates and measurement points for displacement.

In the test, considerable deflection of the girders occurred and, at a load of $Q_{u.exp}$ = 3320 kN (1660 kN for each loading plate), the slab suddenly, without any warning, failed with a combined failure mode of one-way shear and punching shear. The failure was initiated between one of the loading plates and the girder, and propagated on either side of the plate, thus, producing a U-shaped failure surface.

5 Level-of-approximation assessment

The RC bridge deck slab has been evaluated at different assessment levels according to the LoA approach in MC 2010 [8]; following the flow diagram in Figure 4. It starts with a need for an assessment due to changing requirements, deterioration of or damage to the structure. First of all, an initial LoA I assessment based on a study of the documentation, on-site inspection and an analysis using LoA I resistance model should be carried out. If the requirements are fulfilled, i.e. load effect $v_E \leqslant v_{R,c}$, the structure is continue to use. If the requirements are not fulfilled, i.e. load effect $v_E \geqslant v_{R,c}$, the second and third level LoA II & III would continue. A continued assessment can include a linear FE analysis, as well as an improved resistance model based on LoA II & III. If the requirements are not fulfilled, the forth level LoA IV would continue. A continued assessment can include a non-linear FE analysis, as well as an improved resistance model based on LoA II & III; or failure and capacity could be obtained from non-linear FE analysis directly. If the assessment would not continue, the bridge may be demolished, strengthened or subjected to restricted loads for future use. An enhanced assessment may result in a decision whether it would be possible to continue using the bridge, possibly after strengthening or repair, or whether its use might be redefined under intensified monitoring.

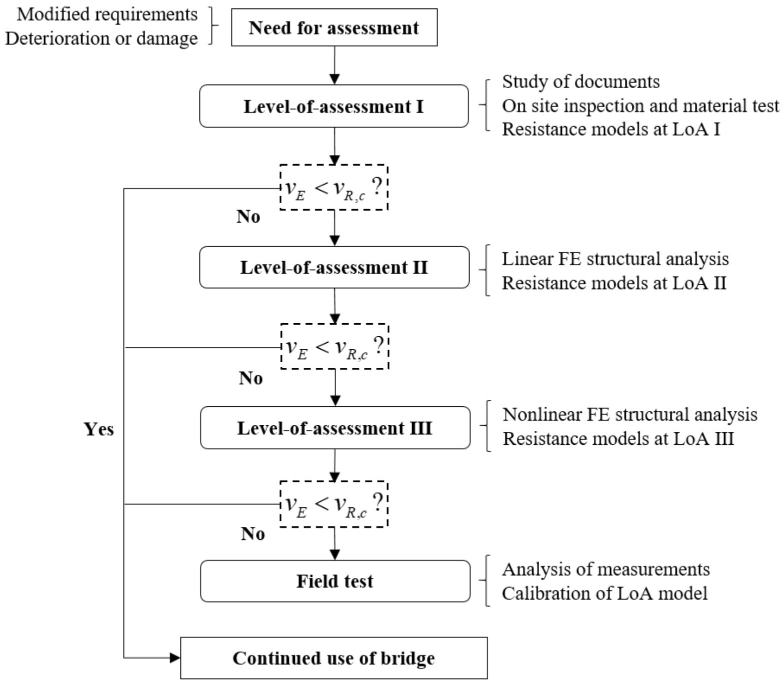

Figure 4. Flow diagram for structural assessment based on the Level-of-Approximation (LoA) approach [8].

For boundary conditions in longitudinal condition it was assumed that the edges were fully fixed since the slab continues over several spans and prestressed in the main girder; see Figure 5. Mean value of material properties were used since safety consideration was not considered and easier to compare the load-carrying capacity at different levels. Only one-way shear and punching shear resistance were assessed since bending and anchorage failures had already been checked and found not to be critical during the design phase of the experiment. The test load setup and dimension of the loading plate is determined according to Load Model 2 in EC 1 [36]. Self-weight was neglected in the calculation because it was very minor compared to the applied load.

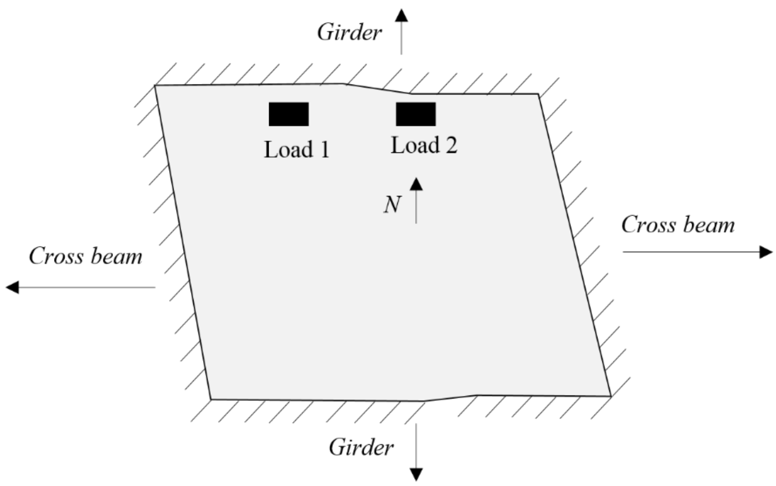

Figure 5. The assumed boundary condition of the bridge deck slab.

5.1 LoA I: Simplified analysis

At an initial level of structural assessment, the load-carrying capacity with respect to one-way shear and punching shear was calculated according to LoA I in MC2010 [8].

For members not requiring design shear reinforcement, the value for the one-way shear resistance follows out of Equations (1) and (2). The critical was taken at the lesser of the distances equal to $a_v/2$ from the face of the support. Since the fixed boundary condition was assumed, the load distribution angle should be taken as $\alpha=45^\circ$ and the arching action should be considered. The factor $\beta = a_v/2d$ to consider arching action was calculated to be 0.62 and 0.5 for the Load 1 and 2 respectively. The choice of effective width has been discussed in Lantsoght et al. [37] and Shu et al. [11].

$$V_R = k_v \sqrt{f_{cm}} b_w z \tag{1}$$

$$k_v = \frac{180}{1000 + 1.25z} \tag{2}$$

k_v is a factor consider the size of the slab; f_{cm} is mean compressive concrete strength; z is effective shear depth of RC slab; b_w refers to the effective width. The length of effective width b_w for one-way shear is shown in Figure 6. Finally, one-way shear resistance resulted to 639 kN for the Load 1 (further) and 723 kN for the Load 2 (closer). Considering when Load 1 was failed, Load 2 cannot take the total load anymore, the total load-carrying capacity in this case is 639 kN × 2 = 1287 kN.

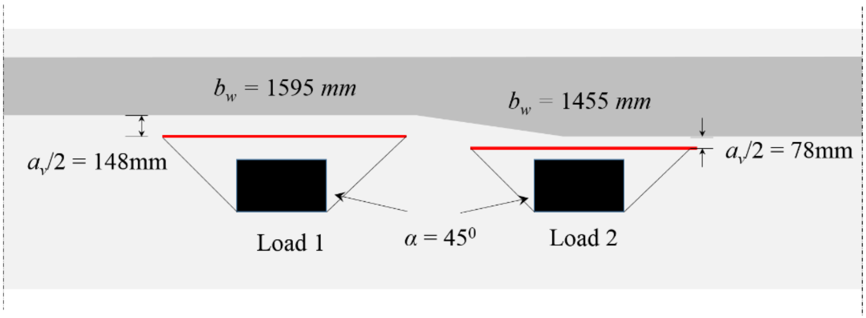

Figure 6: Effective width b_w for calculation of one-way shear resistance.

The punching shear resistance is calculated as the shear per square meter along a control perimeter times the effective depth; see Equations (3) and (4). The basic control perimeter b_1 is measured in a distance of $d/2$ from the supported area and resulted to 2.60 m; see Figure 7. The parameter k_ψ is a function of plate rotation ψ (Equation (6)), member size and maximum grain. There is evidence that the shear resistance of members without shear reinforcement is influenced by the maximum size of the aggregate d_g. If concrete with a maximum size of the aggregate different from d_g = 16 mm is used, the value k_{dg} may be calculated with (5).

It is proposed that the distance from the loading area to the position where the radial bending moment is zero may be assumed as r_s = 0.22 L. However, it is also mentioned that this assumption is only valid for regular slabs where the ratio of the spans in longitudinal and transversal directions is in between 0.5 and 2.0.

$$V_R = k_\psi \sqrt{f_{cm}} b_0 d \tag{3}$$

$$k_\psi = \frac{1}{1.5 + 0.9 k_{dg} \psi d} \tag{4}$$

$$k_{dg} = \frac{32}{16 + d_g} \tag{5}$$

$$\psi = 1.5 \frac{r_s}{d} \frac{f_{ym}}{E_{sm}} \tag{6}$$

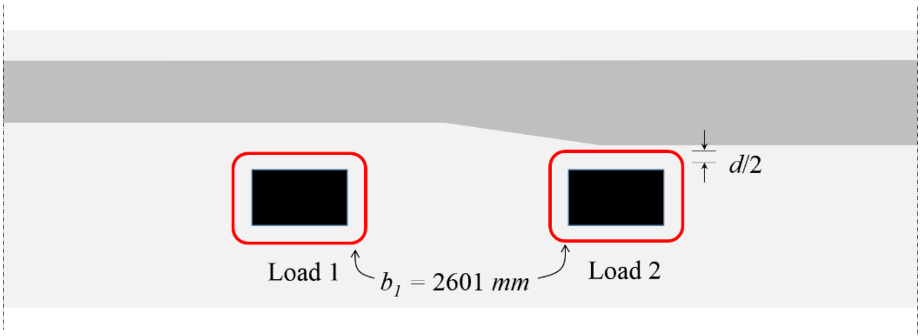

Figure 7. Control perimeter b_1 for calculation of punching shear resistance.

Finally, punching shear resistance resulted to 812 kN for both Load 1 (further) and Load 2 (closer). The total load-carrying capacity in this case is 812 kN × 2 = 1624 kN. At this level, resistance for one-way shear and punching shear was obtained as 1264 kN and 1624 kN respectively.

5.2 LoA II: 3D linear shell (FE) analysis

At level II, a 3D shell element model using software package DIANA 9.6 and Midas FX+ [38] was created in a linear FE analysis to determine the load effects; see Figure 8. For linear analyses a linear relationship between stress and strain is assumed. Therefore, isotropic models for steel and concrete were applied. The material parameters and boundary conditions were used the same as LoA I. The present bridge deck slab was meshed with quadrilateral curved shell elements of size 50 mm × 50 mm. This high mesh density was chosen in order to model the loading area which was close to the side girder as precisely as possible. For describing the slab, in plane a 2×2 Gauss integration scheme was used. In the thickness direction, for linear FE analyses the software automatically divides the slab into three layers.

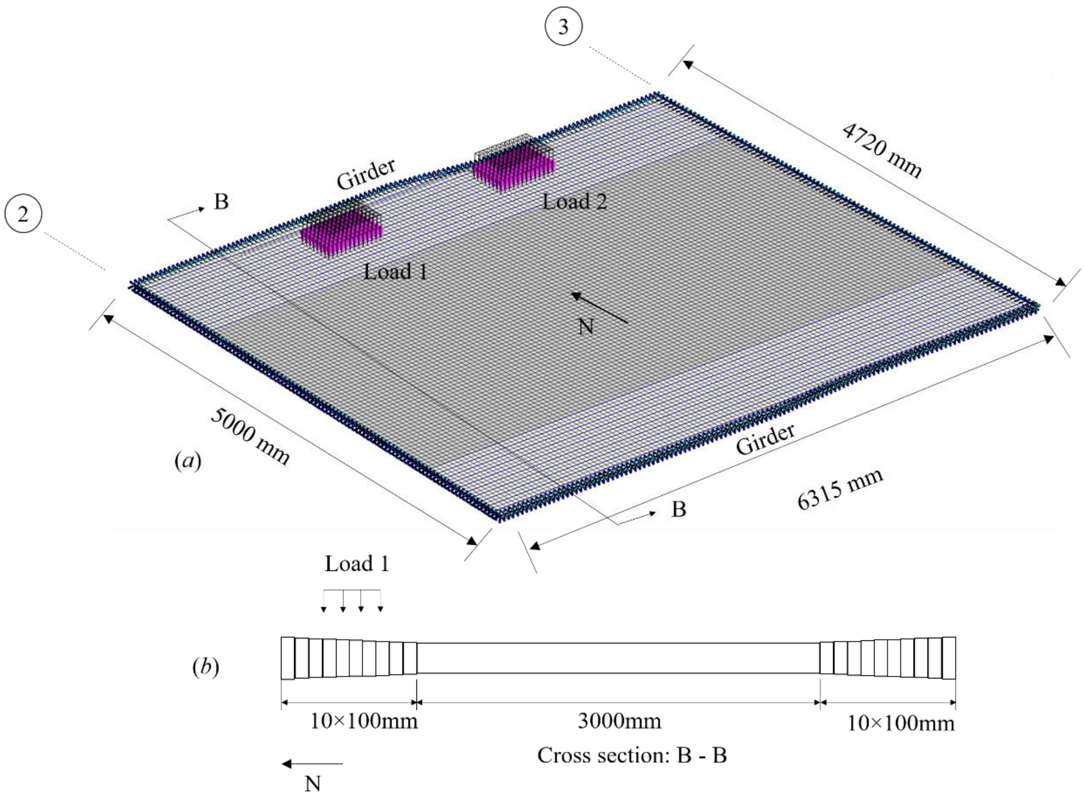

Figure 8. Level II analysis: linear shell FE model of the tested slab (*a*) isometric view of the model; (*b*) cross section of the model; The boundary condition of the slab was assumed to be fixed.

The resistance of one-way shear was still calculated based on (1). However, the value k_v was calculated by (7). The reference strain in transvers direction can be obtained from the FE analysis.

$$k_v = \frac{0.4}{1+1500\varepsilon_x} \cdot \frac{1300}{1000+k_{dg}z} \tag{7}$$

Finally, one-way shear resistance resulted to 737 kN for the Load 1 (further) and 848 kN for the Load 2 (closer). Considering when Load 1 was failed, Load 2 cannot take the total load anymore, the total load-carrying capacity in this case is 737 kN × 2 = 1474 kN.

For punching shear, the applied load was compared to the punching shear resistance calculated according to MC2010 (LoA II) [8]:

$$\psi = 1.5\frac{r_s}{d}\frac{f_{ym}}{E_{sm}}\left(\frac{m_E}{m_R}\right)^{1.5} \tag{8}$$

$$m_R = a_s f_{ym} z = a_s f_{ym}\left(d - \frac{a_s f_{ym}}{2bf_{cm}}\right) \tag{9}$$

$$m_E = V_E \cdot \left(\frac{1}{8} + \frac{|e_{u,i}|}{2 \cdot b_s}\right) \tag{10}$$

where f_{cm} is the mean value of concrete compressive strength, a_s the area of reinforcement per unit width; d is the effective depth of the slab and b_0 is the length of basic control perimeter according to MC2010 [8]. The parameter k_ψ and, hence, the punching resistance depend on the rotations ψ of the slab. Since the rotation ψ depends on the applied load, the load-carrying capacity was determined from the FE analysis and according to equations (8),(9) and (10). V_E is the shear force acting on the slab. m_E is the average moment per unit length for calculation of the flexural reinforcement in the support strip (for the considered direction). In case of non-symmetric conditions, the term $e_{u,i}$ refers to the eccentricity of the resultant of shear forces with respect to the centroid of the basic control perimeter in the direction investigated (i = x and y for x and y directions respectively; see Figure 9).

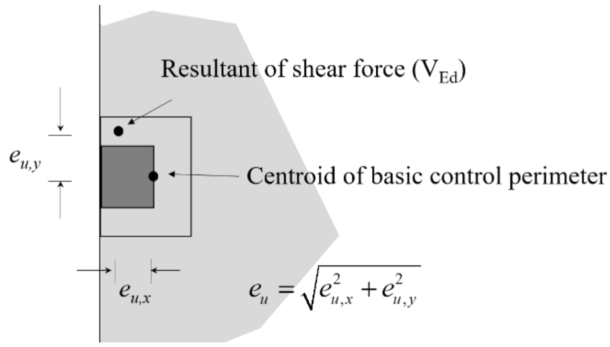

Figure 9. Approximated basic control perimeter for calculation of the position of its centroid and eccentricity between the resultant of shear forces and the centroid of the basic control perimeter [8].

Finally, punching shear resistance resulted to 1160 kN for the Load 1 (further) and 1255 kN for the Load 2 (closer). Considering when Load 1 was failed, Load 2 cannot take the total load anymore, the total load-carrying capacity in this case is 1160 kN × 2 = 2320 kN. At this level, resistance for one-way shear and punching shear was obtained as 1470 kN and 2320 kN respectively.

The benefit of complementing analytical methods with FE analysis is more factors such as geometry and even load distribution can be considered in the calculation. According to MC2010, LoA III does not exist for one-way shear and the circumstance for punching shear was not applicable for this case. Therefore, the analysis will continue with LoA IV instead of LoA III.

5.3 LoA IV: 3D non-linear shell (FE) analysis

At LoA IV, to determine the load effects, the slab was modelled with shell elements using the same FE mesh and integration scheme as in the level II analysis; see Figure 10 (*a*). Moreover, the reinforcement and non-linear behaviour of the materials was also included in the analysis. The vertical loads of traffic were applied to 32 nodes. To enable deformation-controlled loading for several point loads, the loading sub-structure was modelled with very stiff beam elements. The nodes, where the vertical traffic point loads were applied on the steel loading plates on the bridge, were tied to have the same vertical displacements as the corresponding bottom end nodes of the loading arrangement; Figure 10 (*c*). In this way, the load was distributed equally on the nodes of steel plates. The vertical point loads of traffic were applied by increasing the vertical displacement of one node at the top beam element in the loading structure. The analysis was carried out using a regular Quasi-Newton iteration method based on force and energy convergence criteria, with an error tolerance of 0.001. The analysis stopped when convergence could not be achieved due to punching failure. The failure occurred both at material and structural level.

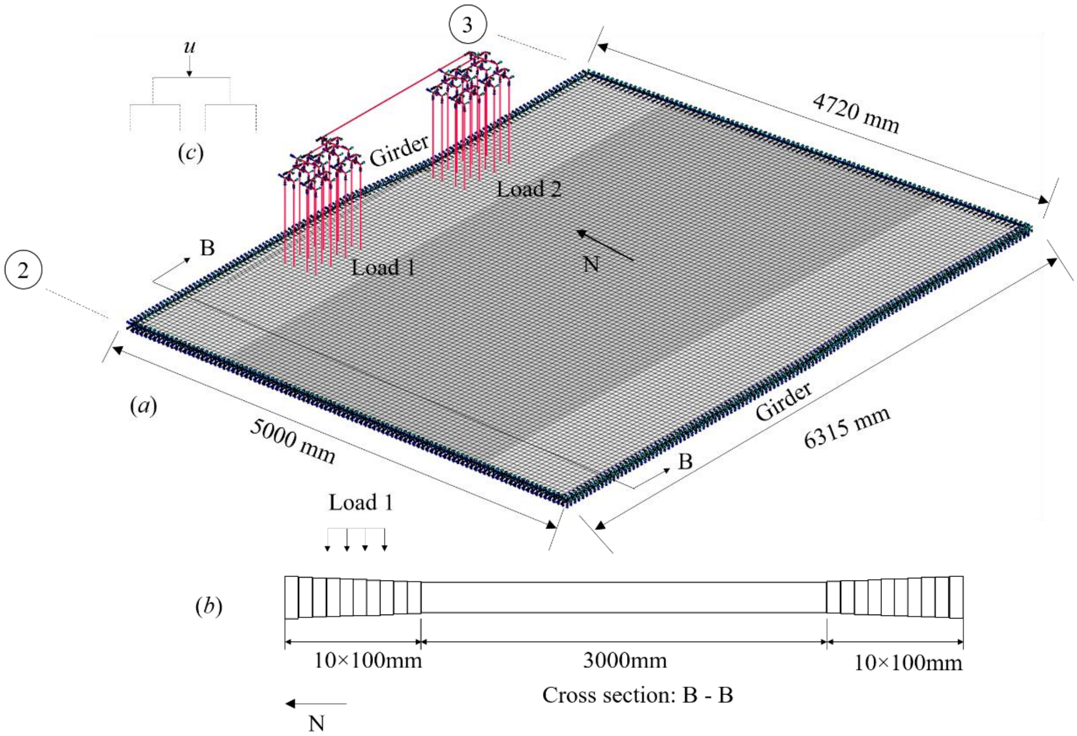

Figure 10. Level IV analysis: non-linear shell FE model of the tested slab (*a*) isometric view of the model; (*b*) principal of loading structure; The boundary condition of the slab was assumed to be fixed.

At LoA IV, more material properties was need, e.g., the tensile strength of concrete and fracture energy, etc. In addition to the in-situ tested material properties, more material parameters were obtained from calculations based on EC2 [5], MC2010 [8] other literatures; For the tensile strength of concrete of the existing bridge, a parameter study has been conducted and reported in another field test of an existing bridge by and Puurula et al. [39] and the method suggested was adopted in this study. Concrete was modelled using a constitutive model based on non-linear fracture mechanics using a smeared rotating crack model based on total strain [38]. In this approach, the crack width w is related to the crack strain $\varepsilon_{t,cr}$ perpendicular to the crack via a characteristic length called crack band width h_b. The advantage of this method is that the formulation remains local and the algorithmic structure of the FE code would require only minor adjustments, limited to the part of the code responsible for evaluations of the stress (and stiffness) corresponding to a given strain increment [40]. The crack band width was assumed to be equal to the mean crack distance, i.e. h_b = 219 mm calculated by EC2 [5], since the reinforcement was modelled as fully bonded, as indicated by Shu et al. [41]. A tension softening curve according to Hordijk [42] was used; see Figure 11 (*a*). It is needed to be mentioned that usually the parameters such as fracture energy is highly unknown in the practice. Fracture energy is calculated to be G_f = 140 Nm/m^2 based on MC2010 [8] considering reduction. In addition, sensitivity analyses have been carried about these parameters (considering the variation) regarding their influence on FE analysis of structures [41]. The values of those assumed material properties has been summarized in Table 2.

Table 2. Assumed material parameters of concrete.

Material parameters	Determination method	Value
Poisson's ratio	MC2010	$v = 0.15$
Tensile strength	MC2010 concerning reduction[39]	$f_{ctm} = 2.0$ MPa
Fracture energy	MC2010 concerning reduction[39]	$G_f = 140$ Nm/m^2
Crack bandwidth	EC2 [5] and Shu et al. [41]	$h_b = 219$ mm

The behavior of concrete in compression was described by an isotropic damage constitutive law. For the stress-strain relationship used in numerical analyses, the localization of deformation in compressive failure needs to be taken into account. The compression softening behavior is related to the boundary conditions and size of the specimen [43].The stress-strain relationship used were based on Thorenfeldt et al. [44], which was calibrated by measurements of compression tests on 300 mm long cylinders. Consequently, the softening branch needed to be modified for the concrete element size used in the FE model. Thus, the stress-strain curve according to Thorenfeldt et al. [44] was modified to fit the concrete element size [45], resulting in a uniaxial stress versus strain response as shown in Figure 11 (*a*). This was done by assuming that the compressive failure would take place in one element row. This assumption was later found to be correct in our analysis. The main difficulty with this method of compression behavior modelling is that the number of elements in which the compressive region will localize is not known in advance. Thus, this assumption needs to be checked when the analysis is finished.

In addition, the effect of cracking parallel to the compression on the compressive behavior and strength of concrete on 3D stress state were also included in the model [46]. The behavior of the reinforcement was described by a von Mises plasticity model, including strain hardening in a bilinear stress-strain relationship, using values obtained from material tests; see Figure 11 (*b*).

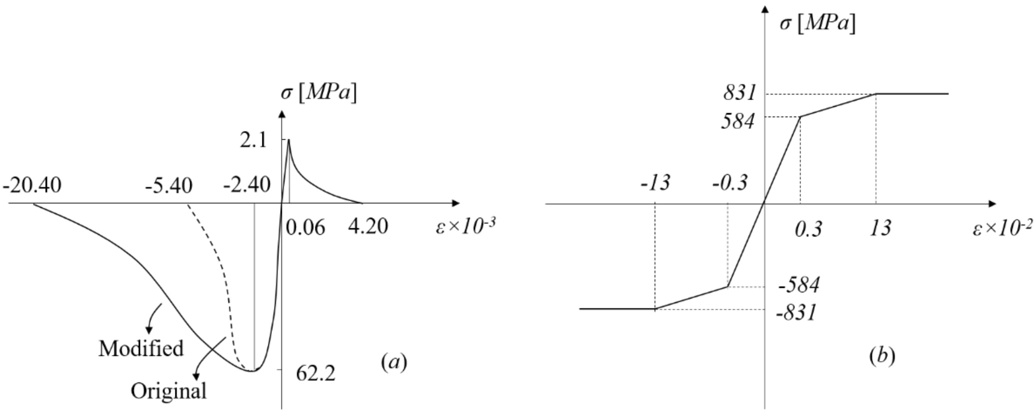

Figure 11. Material model of concrete: (*a*) response of concrete; (*b*) response of reinforcement.

The one-way shear resistance was calculated in the similar way as at level II, according to MC2010 [8]. Compared to LoA II, the advance at LoA IV is that, the shear force from the applied load, transferred over the critical section within effective width, was determined using non-linear FE analysis. Therefore, the redistribution of shear force due to non-linearity (e.g. cracking and plasticity) can be considered in the calculation. The formulation of equitation (1) (2) and (7) is still used, as combined in (11). The external load was increased and the axial strain ε_x was calculated by iteration until shear strength and applied load reached equilibrium.

$$V_R = \left(\frac{0.4}{1+1000\varepsilon_x} + \frac{1300}{1000+k_{dg}z}\right)\sqrt{f_{cm}}\,b_w z \tag{11}$$

Finally, one-way shear resistance resulted to 1100 kN for the Load 1 (further) and 1305 kN for the Load 2 (closer). Considering when Load 1 was failed, Load 2 cannot take the total load anymore, the total load-carrying capacity in this case is 1100 kN × 2 = 2200 kN.

To calculate the punching resistance, the results from the non-linear FE analysis were used coupled with the LoA IV punching shear formulation [8], which was originally developed as Critical Shear Crack Theory (CSCT) [9]. Compared with level II, the rotation ψ can be determined more accurately using FE analysis including non-linear behavior; see Figure 12 (*a*). The rotation the rotation ψ was calculated based on difference of displacement at the center of the girder and center of the loading plate. The punching capacity for loading plate 1 and 2 were checked; the relative shear force resistance is expressed as a function of the rotation ψ of the slab; see Figure 12 (*b*). The load-carrying capacity was then determined as the intersection between this function and corresponding relation between the shear force from the applied load versus slab rotation obtained from the non-linear FE analysis.

The failure criterion for punching shear capacity for loading plate 1 and 2 were checked by the formula [8]:

$$V_R = \frac{1}{1.5 + 0.9\dfrac{32 \cdot \psi \cdot d}{16 + d_g}} b_0 d \sqrt{f_{cm}} \qquad (12)$$

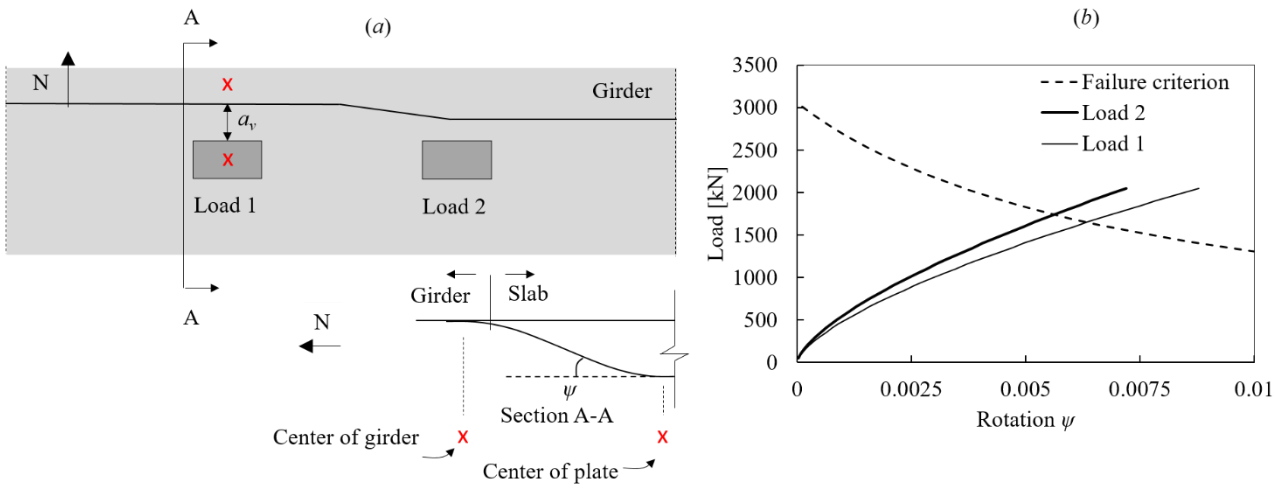

Figure 12. LoA IV analysis: (*a*) non-linear shell FE model of the tested slab and rotation of the slab (*b*) calculations based on LoA IV punching shear formulation.

Finally, punching shear resistance resulted to 1617 kN for the Load 1 (further) and 1750 kN for the Load 2 (closer). Considering when Load 1 was failed, Load 2 cannot take the total load anymore, the total load-carrying capacity in this case is 1617 kN × 2 = 3234 kN. At this level, resistance for one-way shear and punching shear was obtained as 2200 kN and 3234 kN respectively.

6 Results and discussion

Load-carrying capacity and structural behaviour of the bridge deck slab were obtained both from experiment and level-of-approximation approach. The calculated values as well as the key parameters were illustrated in Table 3. A sudden brittle failure took place without any distinct bending cracks observed at the bottom of the slab before the failure. The relative displacement between the slab (measured at D3 and D4 in Figure 3) and the north girder (measured at D1 in Figure 3) is only less than 8 mm. The only sign of the imminent failure was a cracking noise a few seconds before its occurrence. A shear failure was initiated in the slab under loading plate 1 and the girder and finally led to a punching around loading plate 1. Load-deflection relationship from experiment and FE analysis has been presented in Figure 13. (*a*) Load-deflection relationship obtained from field destructive test; (b) load-carrying capacity of the bridge deck slab calculated based on LoA approach and compared with experiment. (*a*).

Table 3. The one-way shear and punching shear capacity of the deck slab calculated using LoA approach is compared to the failure load from the experiment; all the capacity was calculated for Load 1 because it is more critical.

	One-way shear			Punching shear		
	ε_x	k_v	Capacity	ψ	k_ψ	Capacity
Exp.			3320			3320

Level IV	0.00050	0.24	2200	0.0066	0.35	3234
Level II	0.00108	0.16	1474	0.0141	0.23	2320
Level I	0.00125	0.14	1287	0.0206	0.18	1624

The one-way shear and punching shear capacity $Q_{u.cal}$ of the deck slab calculated using LoA approach is compared to the failure load $Q_{u.exp}$ from the experiment in Table 3 and Figure 13 (*b*). At levels I, II and IV, one-way shear capacity and punching shear capacity were calculated according to different resistance models. The comparison is straightforward in Figure 13 (*b*). The one-way shear and punching shear capacity calculated based on LoA at lower level largely underestimated the real capacity. This indicates that the level I and level II model does not fully represent the behavior of the tested bridge deck slab due to different reasons. For instance, the material model used at level I and II did not consider non-linearity, therefore, shear force redistribution was not included. The strain hardening of reinforcement steel was also not included. However, when non-linear FE analysis was adopted with consideration of the non-linearity, the one-way shear and punching shear capacity were predicted closer to the reality.

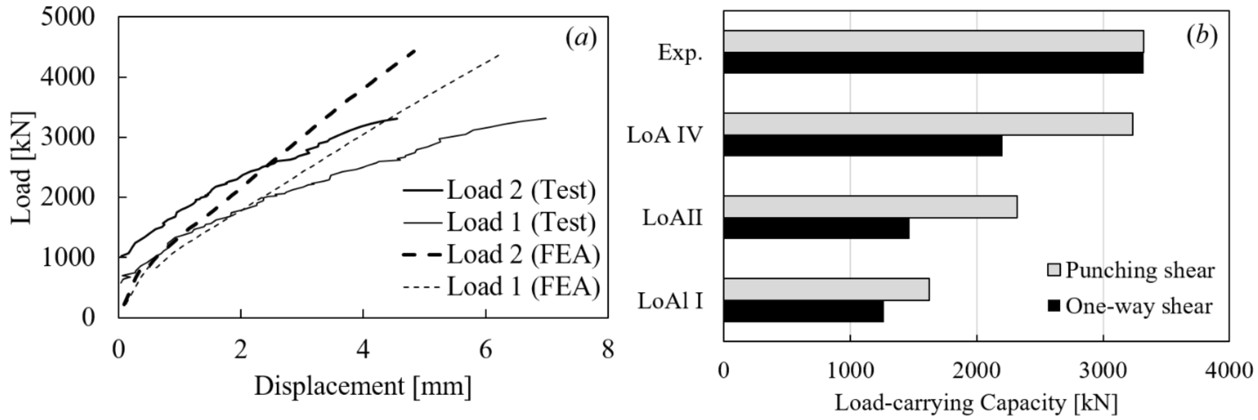

Figure 13. (*a*) Load-deflection relationship obtained from field destructive test; (b) load-carrying capacity of the bridge deck slab calculated based on LoA approach and compared with experiment.

When the punching capacity is calculated for the presstressed girder bridge, compressive membrane action (CMA) usually increase the capacity given the prestressed girders, as indicated in Amir [47] and Belletti et al. [18]. However, even though CMA is considered in building codes, e.g. UK BD81/02 [48] and CHBDC (CAN/CSA-S6-06) [49], it is still difficult, if not possible, to analytically calculate the magnitude of compressive membrane action in lateral restraint slab at lower LoA. Therefore, the CMA has not been considered in the calculation at level I and II. However, since the loading plates are so close to the support, arching action has been considered in the calculation for one-way shear capacity. At higher level of analysis, the CMA is automatically taken into account in the FE analysis by assuming fixed boundary condition.

The crack patterns at the top and bottom of the bridge deck slab after experiment are displayed in Figure 14 (*a*) and (*b*), respectively. The crack pattern actually indicates that the final failure mode was not a pure punching failure, but a combination of one-way shear and punching shear failure. The failure crack developed parallel to the girder and propagated around load 1. It indicates the prediction of failure position by LoA approach is correct. This failure formed a shear type crack that reached the top surface at the edge of the loading plates on the side towards the closest girder, but further away towards the mid-span of the slab, as indicated with a dashed line in Figure 14 (*b*). Whereas, at the bottom surface, a failure crack developed until an U-shaped failure surface around the loading plate 1 was formed. The delamination of the concrete cover was also observed at the bottom of the slab close to the failure surface with the deformation of flexural reinforcement.

(*a*)

(*b*)

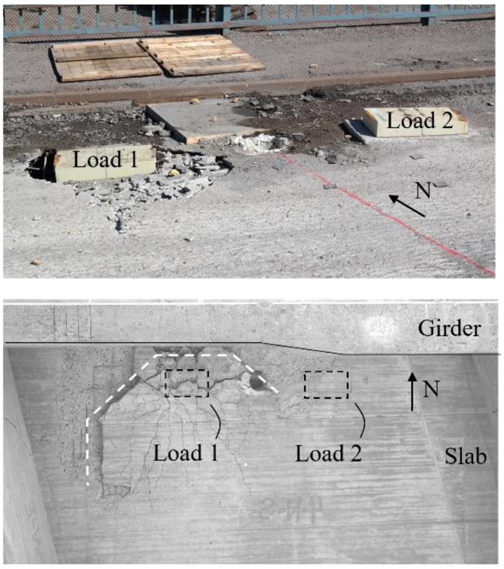

Figure 14. (*a*) Photos of crack pattern after failure at the top of slab in experiment and (*b*) at the bottom of slab.

By the experience and results above, the following recommendations can be provided to the practicing engineers: for the assessment of existing RC bridges deck slabs, it is recommended to use higher level of assessment method if the calculated capacity is not sufficient according to the existing building codes. Those structures is not necessary to strengthen or even replaced if certain marginal capacity can be reflected using advanced assessment method.

As mentioned in literature study, the recommendations for non-linear FE analysis [32] is a good recommendation to the engineering practice for assess safety of general RC structures. The assumptions made in this study also refer to part of the recommendations in the guidelines. In comparison, the assumption is this study is more specific to the RC slabs and can be a seen as a complement to the existing non-linear FE analysis guidelines.

7 Summary and conclusions

The aim of this study is to examine the levels-of-approximation (LoA) approach, introduced in fib Model Code for Concrete Structures 2010 (MC2010) [8], for analysis of the RC bridge deck slabs. The different levels include simplified calculation method, linear finite element analysis as well as non-linear finite element analysis. The differences between analysis methods at different levels of analyses was discussed regarding one-way shear and punching shear behavior of the slab. Based on performed studies the following conclusions can be drawn:

It can be concluded that the LoA approach can provide successively improved evaluation in structural assessment. In general, assessment at lower levels yields too conservative load-carrying capacity and assessment at higher level is more accurate compared to the reality.

It can be determined from the field test, the bridge deck slab failed in a brittle manner without any distinct bending cracks observed at the bottom of the slab before the failure. The relative displacement between the slab and the supporting girder is minor. A combined failure mechanism took place, initiated with an one-way shear coupled with a secondary punching failure.

The application of non-linear shell element FE analysis for calculation of slab rotation in combination with the LoA IV delivered accurate results. However, especially if loads were placed close to the support, the gained results have to be evaluated critically. An appropriate choice of boundary conditions should be considered.

8 Acknowledgements

This project is funded by Chalmers University of Technology. The author would like to express his outmost gratitude to the financers, supervisors and colleagues at Chalmers for contributions and making this research possible. The authors also would like to acknowledge the support from The Swedish Transport Administration (Trafikverket) and colleagues from Luleå University of Technology (LTU).

9 References

1. SB-LRA. Guideline for Load and Resistance Assessment of Existing European Railway Bridges. Sustainable Bridges: Report; 2007.
2. Shu J, Zhang Z. Damage detection on railway bridges using Artificial Neural Network and train-induced vibrations. [Stockholm, Sweden]: Master Thesis, Royal Institute of Technology; 2012.
3. SB-ICA. Guideline for Inspection and Condition Assessment. Sustainable bridges: Report; 2007.
4. ACI. Building Code Requirements for Structural Concrete and Commentary. Farmington Hills, Mich: ACI American Concrete Institute; 2014.
5. CEN. Eurocode 2: Design of concrete structures - part 1-1: General rules and rules for buildings. Brussels, Belgium: CEN European Committee for Standardization; 2004.
6. Plos M, Shu J, Zandi K, Lundgren K. A multi-level structural assessment strategy for reinforced concrete bridge deck slabs. Struct Infrastruct Eng. 2016;13(2):223–41.
7. Honfi D, Leander J, Björnsson Í. Decision support for bridge condition assessment. In: The fourth international conference on Smart Monitoring, Assessment and Rehabilitation of Civil Structures (SMAR 2017). Zürich, Switzerland; 2017.
8. fib. Model Code for Concrete Structures 2010. Lausanne: International Federation for Structural Concrete (fib); 2013.
9. Muttoni A. Punching Shear Strength of Reinforced Concrete Slabs. ACI Struct J. 2009;(105):440–50.
10. Shu J, Belletti B, Muttoni A, Scolari M, Plos M. Internal force distribution in RC slabs subjected to punching shear. Eng Struct. 2017;153:766–81.
11. Shu J, Bagge N, Plos M, Johansson M, Yang Y, Zandi K. Shear and Punching Capacity of a Field Failure Tested RC Bridge Deck Slab. ASCE J Struct Eng. 2017;(Accepted).
12. Lantsoght EOL, Boer A de, Veen C van der. Levels of Approximation for the shear assessment of reinforced concrete slab bridges. Struct Concr. 2016;1.
13. Fischer O, Lechner T, Wild M, Müller A, Kessner K. Re-analysis of concrete bridges – systematic data evaluation of re-analysed concrete bridges. Brücken- und Ingenieurbau H B. 2016;124(66):(In German).
14. Marzahn G. About the provisions for evaluating necessary upgrades of older road bridges. Beton- und Stahlbetonbau. 2011;106(11):730–735 (In German).
15. Huber P, Schweighofer A, Kollegger J, Brunner H, Karigl W. Comparison of the calculative shear resistance of existing bridges according to Eurocode 2 and fib Model Code 2010. Beton- und Stahlbetonbau. 2012;107(7):451–462 (In German).
16. Slowik O, Novak D, Krug B, Strauss A. Shear failure of pre-stressed concrete T-shaped girders: experiment and nonlinear modeling. In: IABSE Conference 2015 – Structural Engineering: Providing Solutions to Global Challenges. Geneva, Switzerland; 2015. p. 1137–47.
17. Nilimaa J, Blanksvärd T, Täljsten B. Assessment of concrete double-trough bridges. J Bus Psychol. 2015;30(1):29–36.
18. Belletti B, Walraven JC, Trapani F. Evaluation of compressive membrane action effects on punching shear resistance of reinforced concrete slabs. Eng Struct. 2015;95:25–39.
19. Belletti B, Damoni C, Hendriks M, Boer A de. Analytical and numerical evaluation of the design shear resistance of reinforced concrete slabs. Struct Conrete. 2014;317–30.
20. Belletti B, Pimentel M, Scolari M, Walraven JC. Safety assessment of punching shear failure according to the level of approximation approach. Struct Concr. 2015;16(3):366–80.
21. Guandalini S, Burdet OL, Muttoni A. Punching tests of slabs with low reinforcement ratios. ACI Struct J. 2009;87–95.
22. Bonić Z, Davidović N, Vacev T, Romić N, Zlatanović E, Savić J. Punching Behaviour of Reinforced Concrete Footings at Testing and According to Eurocode 2 and fib Model Code 2010. Int J Concr Struct Mater. 2017;11(4):657–76.
23. Ricker M, Häusler F, Randl N. Punching strength of flat plates reinforced with UHPC and double-headed studs. Eng Struct. 2017;136:345–54.
24. Clément T, Ramos AP, Ruiz MF, Muttoni A. Design for punching of prestressed concrete slabs. Struct Concr. 2013;14(2):157–67.
25. Ruiz MF, Navarro MG, Bamonte P. Fire design of concrete structures based on a levels-of-

approximation approach. In: 2015 fib Symposium: Concrete - Innovation and Design; Tivoli Congress CenterCopenhagen; Denmark. Copenhagen; 2015.

26. Micallef K, Sagaseta J, Ruiz MF, Muttoni A. International Journal of Impact Engineering Assessing punching shear failure in reinforced concrete fl at slabs subjected to localised impact loading. 2014;71.

27. Menétrey P. Relationships between Flexural and Punching Failure. Struct J. 1998;95(4).

28. Hallgren M. Punching shear capacity of reinforced high-strength concrete slabs. [Stockholm]: Doctoral Thesis, Royal Institute of Technology in Stockholm (KTH); 1996.

29. Marzouk H, Chen Z. Finite element analysis of high strength concrete slabs. ACI Struct J. 1993;90:505–13.

30. Polak A. Modeling Punching Shear of Reinforced Concrete Slabs Using Layered Finite Elements. ACI Struct J. 1998;95(1):71–80.

31. Shu J, Plos M, Johansson M, Zandi K, Nilenius F. Prediction of punching behaviour of RC slabs using continuum non-linear FE analysis. Eng Struct. 2016;

32. Hendriks M, Boer A de, Belletti B. Guidelines for Nonlinear Finite Element Analysis of Concrete Structures. 2016.

33. Miller R, Aktan AF, Shahrooz BM. Destructive Testing of Decommissioned Concrete Slab Bridge. ASCE J Struct Div. 1994;120(7):2176–98.

34. Pressley J, Candy C, Walton B, Sanjayan J. Destructive Load Testing of Bridge No . 1049 – Analyses , Predictions and Testing. In: Fifth Austroads Bridge Conference, Hobart, Tasmania. Austroad; 2004.

35. Lantsoght EOL, Yang Y, van der Veen C, de Boer A, Hordijk DA. Ruytenschildt Bridge: Field and laboratory testing. Eng Struct. 2016;128:111–23.

36. CEN. Eurocode 1 - Actions on structures - Part 2 - Traffic loads on bridges. Brussels, Belgium: CEN European Committee for Standardization; 2003.

37. Lantsoght E, Veen C, Walraven J. Shear in One-Way Slabs under Concentrated Load Close to Support. ACI Struct J. 2014;(110):275–84.

38. TNO. Diana finite element analysis, User's Manual -- Release 9.6. TNO DIANA BV. Delft; 2015.

39. Puurula AM, Enochsson O, Sas G, Blanksvärd T, Ohlsson U, Bernspång L, et al. Assessment of the Strengthening of an RC Railway Bridge with CFRP Utilizing a Full-Scale Failure Test and Finite-Element Analysis. 2015;141(1):1–11.

40. Jirásek M. Modeling of localized inelastic deformation. Prague: Czech Technical University in Prague; 2012. 137-139 p.

41. Shu J, Fall D, Plos M, Zandi K, Lundgren K. Development of modelling strategies for two-way RC slabs. Eng Struct. 2015;101:439–49.

42. Hordijk DA. Local approach to fatigue of concrete.pdf. [Delft, Netherlands]: Delft University of Technology; 1991.

43. Mier J. Strain-softening of concreie under multiaxial loading conditions. [Eindhoven]: Doctoral Thesis, Eindhoven University of Technology; 1984.

44. Thorenfeldt E, Tomaszewicz A, Jensen JJ. Mechanical properties of high-strength concrete and applications in design. In: In Proc Symp Utilization of High-Strength Concrete. Stavanger; 1987.

45. Zandi Hanjari K, Kettil P, Lundgren K. Modeling the Structural Behavior of Frost-damaged Reinforced Concrete Structures. Struct Infrastruct Eng. 2013;9(5):416–31.

46. Vecchio FJ, Collins MP. Compression response of cracked reinforced concrete. J Stru. 1994;119(12):241–8.

47. Amir S. Compressive membrane action in prestressed concrete deck slabs. [Delft]: PhD Thesis. Delft University of Technology; 2014.

48. 81/02 UKAB. Use of compressive membrane action in bridge decks. Design manual for roads and bridges. 2002. 3. p. 11.1–11.5.

49. S6-06 C. CAN/CSA S6-06 - Canadian Highway Bridge Design Code. Canadian Standard Association;